Plant Soil (2011) 340:169–180
DOI 10.1007/s11104-010-0448-5

REGULAR ARTICLE

Grazing effects on seasonal dynamics and interannual variabilities of spectral reflectance in semi-arid grassland in Inner Mongolia

Liya Fan · Bettina Ketzer · Huizhi Liu · Christian Bernhofer

Received: 31 December 2009 / Accepted: 21 May 2010 / Published online: 9 June 2010

Abstract Detecting the influences of land management on seasonal dynamics and interannual variabilities of grassland surface reflectance is of scientific and practical importance as it can help to monitor grazing effects on the grassland ecosystem. We conducted spectral reflectance measurements at five differently grazed sites in Inner Mongolia, China, during the growing seasons of 2005 and 2006 using a portable, highly resolving spectrometer. Through analyses of the measured surface reflectance spectra and the derived visible albedo and NDVI, we found that grazing influences the reflectance spectrum shape and affects the visible albedo and NDVI seasonal pattern; visible albedo and NDVI of grazed sites are more sensitive to precipitation than that of ungrazed sites. In addition, we observed a well-defined linear relationship between total shortwave and visible (PAR) albedo, with R= 0.83 and R=0.94 for 2005 and 2006, respectively, and between NDVI and total shortwave albedo with R=−0.92. Thus, NDVI spectrometer measurements and total shortwave albedo pyranometer measurements are interchangeable when addressing different grazing intensities.

Keywords Grazing · Semi-arid grassland · Spectral reflectance · Seasonal dynamics · Interannual variabilities

Responsible Editor: Ingrid Koegel-Knabner.

L. Fan (✉) · B. Ketzer · C. Bernhofer
Department of Meteorology,
Institute of Hydrology and Meteorology,
Technische Universität Dresden,
01737 Tharandt, Germany
e-mail: lyfan77@hotmail.com

B. Ketzer
e-mail: bettina.ketzer@forst.tu-dresden.de

C. Bernhofer
e-mail: christian.bernhofer@tu-dresden.de

H. Liu
Institute of Atmospheric Physics,
Chinese Academy of Sciences,
100029 Beijing, China
e-mail: huizhil@mail.iap.ac.cn

Abbreviations

UG79	site not grazed since 1979
UG99	site not grazed since 1999
WG	winter grazed site
CG	continuously and moderately grazed site
HG	heavily grazed site

Introduction

Surface spectral reflectance is a basic key parameter for vegetated surfaces such as forest, grassland and

agricultural land. From this value, the biophysical and biochemical parameters of vegetation can be assessed, including leaf chlorophyll and N contents (Yoder and Pettigrew-Crosby 1995; Boegh et al. 2002; Huang et al. 2004; Houborg and Boegh 2008), leaf area index (LAI), fraction of absorbed photosynthetically active radiation (fPAR) (Leblon et al. 1991; Knyazikhin et al. 1998; Vaesen et al. 2001; Colombo et al. 2003) and even net primary production (NPP) and evapotranspiration (Elvidge and Chen 1995; Higuchi et al. 2000; Pineiro et al. 2006).

In addition to estimating vegetation properties, surface spectral reflectance is also used in the discrimination of land management and degradation of grassland. Price et al. (2002) and Guo et al. (2003) reported discrimination of different grassland management practices in the Kansas Prairie using the Landsat Thematic Mapper (TM) data. Liu et al. (2004) assessed the grassland degradation near Lake Qinhai in west China using TM images and in situ measurements; Kawamura et al. (2005) developed a methodology for quantifying the effects of grazing intensities on plant biomass using the normalised difference vegetation index (NDVI) obtained with a moderate resolution imaging spectroradiometer (MODIS) in the Xilingol steppe region, Inner Mongolia, China. Wang (1998, 2001) also studied the influence of grazing intensity on spectral reflectance in Inner Mongolia through in situ measurements.

These studies were mainly focused on the assessment of grassland status through spectral reflectance, but few involved the detection of grassland dynamics by land management using spectral reflectance. As inappropriate human activities such as overgrazing are one of the most important reasons for land degradation and desertification of grassland (Li et al. 2000), detecting the influences of land management on seasonal dynamics and interannual variabilities of grassland surface reflectance is of scientific and practical importance. In this paper, we conducted spectral reflectance measurements at five differently grazed grasslands in Inner Mongolia, China during the 2005 and 2006 growing seasons by a portable, highly resolving spectrometer, with the aim of studying grazing effects on grassland surface reflectance seasonal dynamics and interannual variabilities. This work aids in the understanding of grazing effects, particularly the effects of heavy grazing on the grassland ecosystem.

Materials and methods

Study sites

The study area is in a typical steppe ecosystem south of the Xilin river catchment, located in northeastern Inner Mongolia, China (Fig. 1). It is adjacent to the Inner Mongolia Grassland Ecosystem Research Station (IMGERS, 43°38′N, 116°42′E) of the Chinese Academy of Sciences. The average elevation is approximately 1,200 m, with a gentle slope of 2~4°. The climate belongs to a semi-arid monsoon climate in a temperate zone. The mean annual precipitation is approximately 350 mm, mainly occurring from June to August. The mean annual temperature is 1.0°C. The mean growing season lasts approximately 150 days (Jiang 1985).

Five experimental sites with different sheep grazing intensities and land treatment histories were selected (Fig. 1, areas with 15-m grid, Archer 2004a). Two areas have been fenced and have not been grazed since 1979 and 1999, respectively. The other areas are grazed sites; one is a winter grazed area, with grazing from mid-October to mid-February, another area is continuously and moderately grazed throughout the year, with a grazing intensity of approximately 1.6 sheep per hectare, and the last area is heavily grazed, with a grazing intensity of approximately 4 sheep per hectare (Archer 2004b). All sites (named UG79, UG99, WG, CG and HG, respectively; always mentioned in this order) have a main soil type of dark chestnut, and vegetation types are categorised as *Leymus chinensis* and *Stipa grandis* communities.

Ground measurements

Field campaigns of surface spectral reflectance measurements were conducted at the five grasslands from May to September 2005 and from August to September 2006 with a portable spectrometer (getSpec-PDA-UV/VIS, www.getspec.com) with a spectrum range of 380–1,100 nm, a resolution of 0.2 nm and a high signal-to-noise ratio of 12000:1.

At each site, a representative measurement plot of 120×150 m was selected (Fig. 1). Reflectance spectra were measured at 5–6 points around the centre of the plot with a 30-m distance from the centre, according to a geostatistically designed protocol (Archer 2004a). A calibrated white reference (Spectralon, Labsphere)

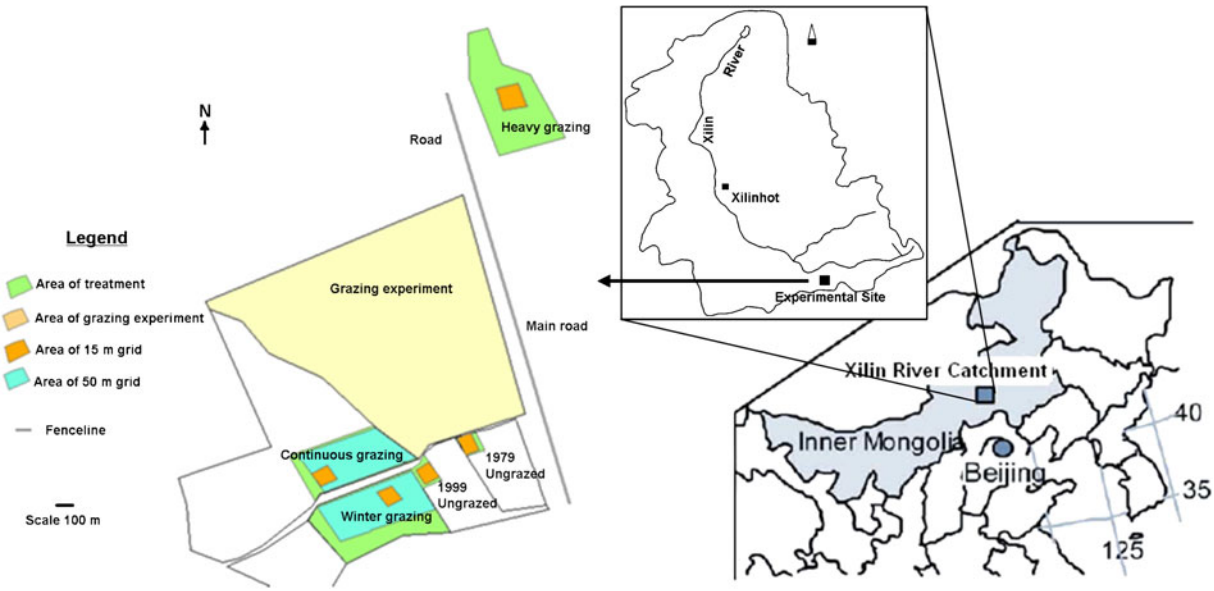

Fig. 1 Location of Xilin River catchment and the measurement sites (left panel from Archer 2004a)

was also measured at each point. The optical fibre platform and white reference platform were both levelled before each measurement. Spectral reflectance was derived as the ratio of reflected radiance by grassland to incident radiance by the white reference panel. The average reflectance of these 5–6 points was used to represent the mean reflectance of each site. All measurements were carried out under clear sky conditions near midday.

Data analysis

Grazing effects on surface properties are first analysed with reflectance spectra, and then further analysed with the derived visible albedo and NDVI parameters from the spectra. Analyses are conducted with supporting information of weekly vegetation height and percent green cover (recorded by measuring tape and estimated by visual judgment, respectively), daily precipitation and air temperature and soil moisture.

Like the method for validating Landsat reflectance by ground spectral measurements (Liang et al. 2002a), spectral reflectances at the central wavelength of Landsat TM bands were used to derive visible albedo and NDVI:

$$\alpha_{vis} = 0.443\alpha_1 + 0.317\alpha_2 + 0.240\alpha_3 \quad (1)$$

where α_i (i = 1, 2, and 3) represent surface spectral reflectance of TM bands 1, 2, and 3 (450–510 nm, 520–600 nm and 630–690 nm, respectively. Liang 2000; Liang et al. 2002b);

$$NDVI = (r_4 - r_3)/(r_4 + r_3) \quad (2)$$

where r_3 and r_4 are the surface spectral reflectances of TM bands 3 and 4 (750–900 nm).

Results

Reflectance spectra

Figures 2 and 3 illustrate the reflectance spectra at each site in 2005 and 2006, respectively, and Table 1 presents the vegetation status during the entire growing season at site UG79 in 2005. In total, there were six measurement campaigns of reflectance spectra in 2005, on May 24, June 3, July 6, August 2, August 17, and September 19 (the uneven measurement frequency is due to weather conditions), and seven measurement campaigns were conducted in August and September 2006, on August 3, 9, 14, 16, and 21, and September 2 and 17.

In 2005, the reflectance spectrum on May 24 showed the highest reflectivity among the six measurements for all sites, because in late May, the grass

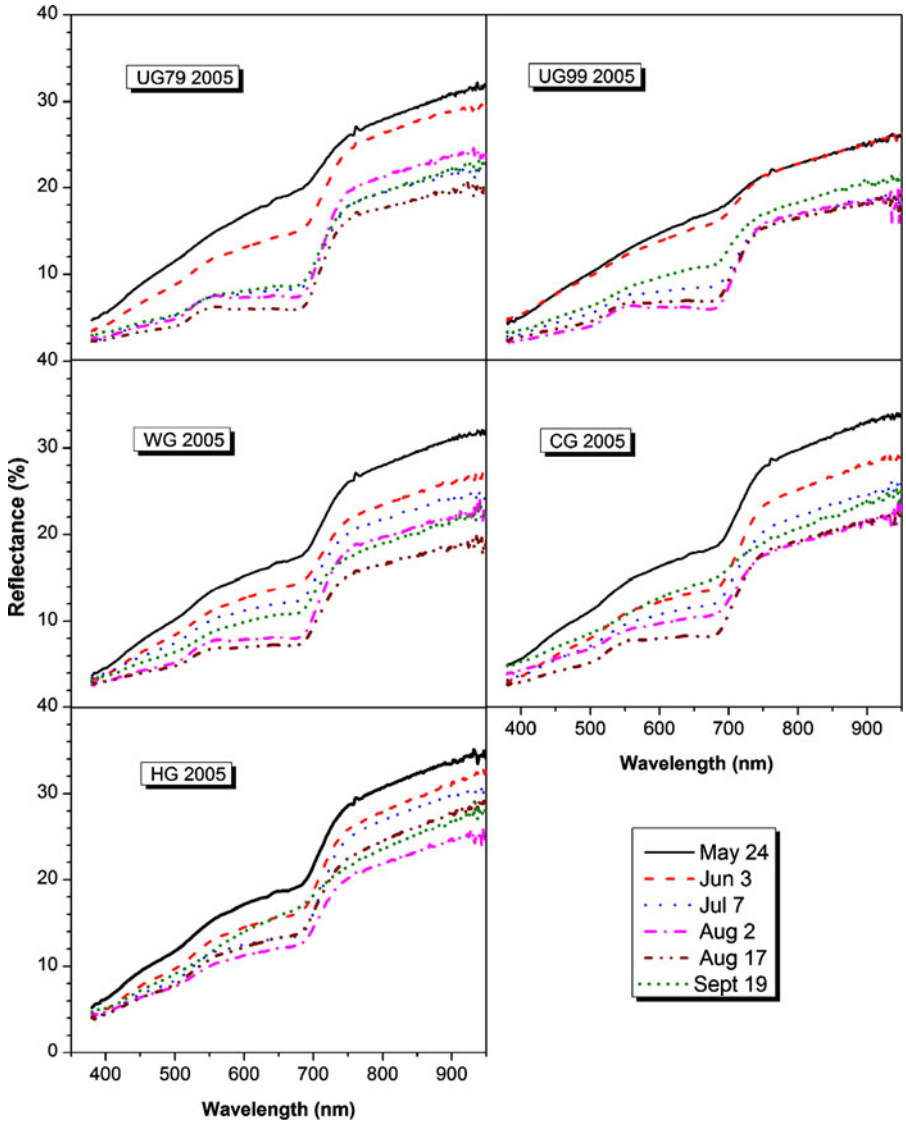

Fig. 2 Seasonal variation of the reflectance spectrum in 2005 at each site (UG79, UG99, WG, CG and HG)

is still in the initial growth phase (Li et al. 1990), and vegetation height and percent green cover (P_v) are relatively low (Table 1). On June 3, the reflectance spectrum declined remarkably at nearly all sites. From Table 1, we know that grass grew higher and denser in early June; thus, more radiation was absorbed by the canopy vegetation, leading to declined surface reflectance.

In July and August, all reflectance spectra declined further, and the chlorophyll red edge (the transitional slope from red to near-infrared light, Tucker 1979; Jackson et al. 1983) increased in slope and height, indicating more absorption of visible light but more reflection of near-infrared light, meaning high NDVI (see Eq. 2). Table 1 shows that in this stage, the vegetation height and percent green cover both gradually reached peak values. The clear chlorophyll red edge is a signal of increasing chlorophyll content. The shoulder peak appearing at the green band of the reflectance spectrum is a further indicator, as chlorophyll absorbs radiation in blue and red bands but reflects in the green band (Gates et al. 1965). From Fig. 2 it also can be seen that the chlorophyll red edge change was particularly pronounced at sites UG79 and UG99.

On September 19, the reflectance spectrum at each site rose, the chlorophyll red edge became blurred, and the peak reflection at the green band almost

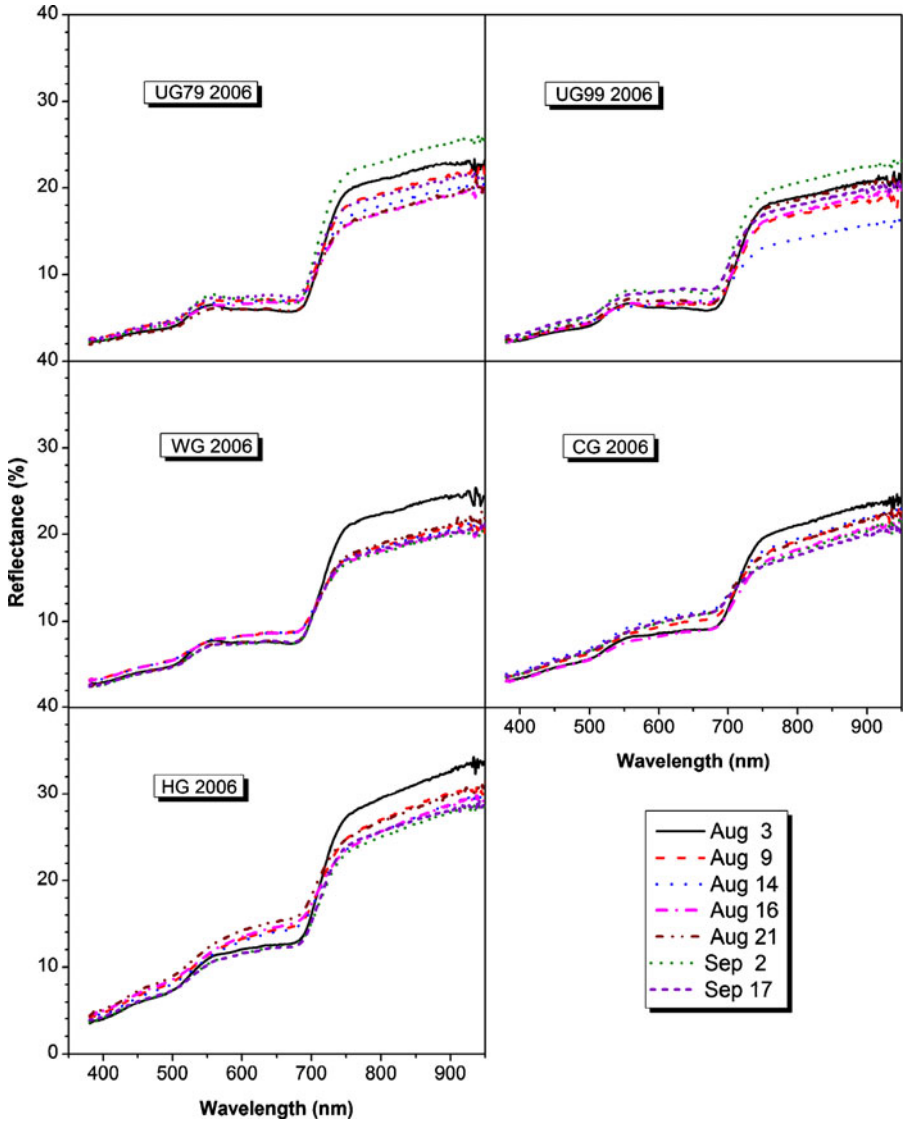

Fig. 3 Seasonal variation of the reflectance spectrum in 2006 at each site (UG79, UG99, WG, CG and HG)

disappeared. These changes were particularly noticeable at sites CG and HG. According to the climate in the study area, air temperature starts to decline in late August, accelerating its decline in September (Li et al. 1990); thus, the vegetation withers rapidly, and the percent green cover and chlorophyll content drops dramatically.

Table 1 Vegetation height (H, cm) and percent green cover (P_v, %) at UG79 in 2005

Date	May 30	June 7	July 5	August 1	August 15	Sep. 19
H	15.4	16.1	19.9	24.5	27	~27.0
P_v	20	30	40	50	60	10

In 2006, the reflectance spectra looked similar due to the short time interval between each measurement, and the differences in spectra between August and September were small. Meteorological data (Fig. 4) indicated minor differences in temperature between the two years (aside from the snow period of September 7 and 8, 2006), but there was higher precipitation in 2006, especially in September (total precipitation was 47.6 mm until September 22, which is much higher than in 2005). This indicates that with favourable growth conditions, vegetation in 2006 was

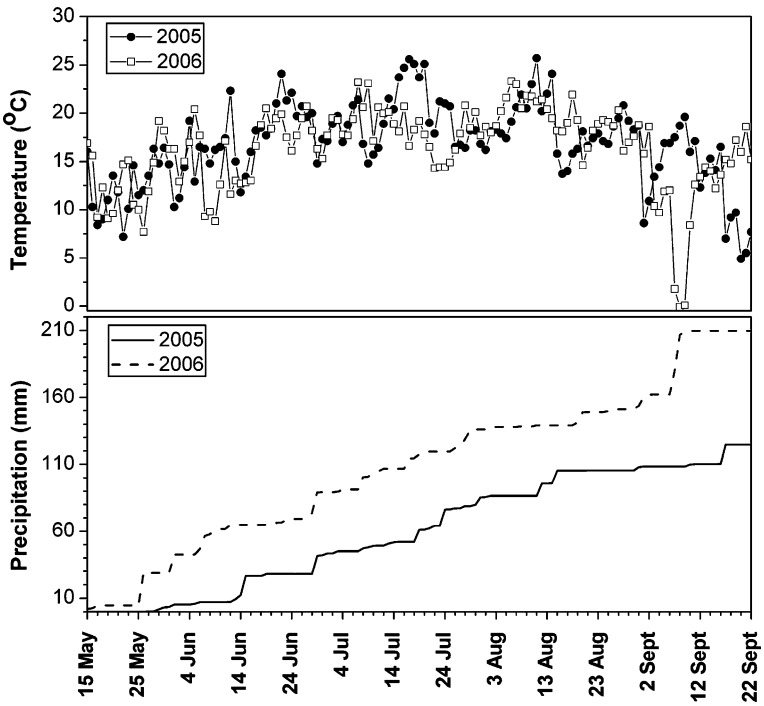

Fig. 4 Daily air temperature and precipitation during the growing season in 2005 and 2006 (from May 15 to September 22)

growing well until late September. The ground survey also shows that the percent green cover at site UG79 on September 16 was nearly 20% higher than the corresponding time period in 2005 (September 19).

Visible albedo

Quantitative estimation of reflectivity in the visible part of the spectrum is obtained by visible albedo (Eq. 1). Figure 5 shows the visible albedo at the five sites in 2005 and 2006.

The time series of visible albedo in 2005 shows a "U" shape pattern at each site (Fig. 5a), which is consistent with the spectrum change analyzed above; the highest visible albedo appeared in May, was lowest in August, and increased again in September.

From Fig. 5a, it can be seen that site UG79 had the biggest variation of visible albedo, and site HG had the smallest variation. In addition, HG had the highest visible albedo among the five sites during the entire growing period. It can be also observed from Fig. 5a that the differences in visible albedo among the five sites were relatively small at the beginning of the growing season (May 24 to June 3), but gradually became more distinct and were greatest in late August (August 17).

The visible albedo in 2006 (Fig. 5b) showed more fluctuation. As reported by Duchon and Hamm (2006), the correlation between albedo and precipitation is such that rainfall can lead to a decrease in albedo and vice versa. The changes in albedo are a consequence of darkening with wetting of the soil and brightening with drying of the soil. On the other hand, rainfall can probably help to remove the dust from vegetation and can trigger (re)growth afterward, therefore resulting in low albedo. From precipitation data shown in Fig. 4, we know that there was only 1.3 mm of rainfall from August 3 to 18 in 2006. Therefore, the visible albedo ascended roughly at most of the sites during this time (measurement error may exist in the CG site plot on August 16); therefore, on August 16, the visible albedo at most of the sites was higher than that for the corresponding time period in 2005 (August 17; visible albedo differences between two years for the five sites are 0.005, −0.001, 0.01, 0.005, and 0.009, respectively), as the rainfall during this period in 2005 was 18.7 mm.

After the snow period on September 7 and 8, the response of visible albedo to precipitation became more evident: instead of being higher, the visible albedo on September 17 at all sites was nearly the same as on September 2. For this reason, the visible

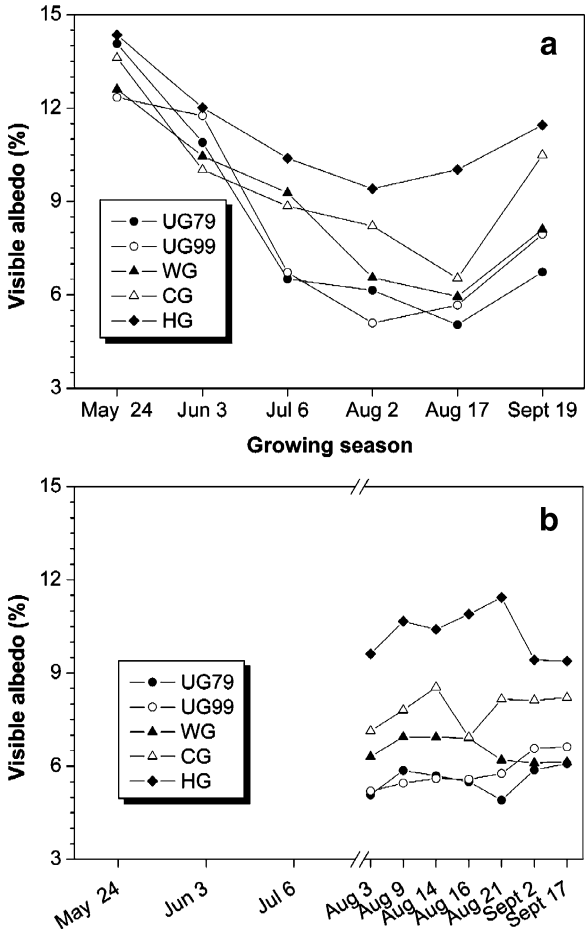

Fig. 5 Seasonal variation of visible albedo in 2005 (**a**) and 2006 (**b**) at each site (UG79, UG99, WG, CG, and HG)

albedo on September 17 for all sites was much lower than that for the corresponding time period in 2005 (September 19, with relatively large differences of 0.006, 0.013, 0.020, 0.023, and 0.021, respectively). From the interannual difference at each site, we can see that the visible albedo at grazed sites is more sensitive to precipitation. Again, in 2006, site HG showed the highest visible albedo among the five sites for all measurements.

Figure 6 and Table 2 provide the mean visible albedo at each site in 2005 and 2006. Site UG79 had the lowest value among the five sites. The values at the other sites were 1.003, 1.072, 1.168, and 1.369 times the value of site UG79 in 2005, and 1.05, 1.17, 1.41, and 1.84 times in 2006, indicating that heavier grazing intensity is correlated with higher visible albedo and that the grazing effect is much clearer in the data for 2006.

Because of the limited spectrum range of the spectrometer, only the visible albedo was obtained in this study. Nevertheless, the total shortwave albedo measurements at site UG79 and the other sites (rotated every 6 weeks, measured by Kipp and Zonen CNR1 pyranometer installed at eddy covariance (EC) tower) during the field campaign make it possible to investigate the correlation between both kinds of albedo.

As illustrated in Fig. 7, the total shortwave albedo was much higher than the visible albedo due to high reflectance in the near-infrared band, but both albedo parameters showed similar variations during the growing season and similar relationships between sites. The linear correlation coefficient (R) of both albedo parameters was 0.83 and 0.94 in 2005 and 2006, respectively.

NDVI

By employing Eq. 2, NDVI was obtained from the measured reflectance spectra. NDVI is an indicator of vegetation growth. High NDVI means well-developed vegetation, high percent green cover, and high above-ground biomass.

Figure 8 shows the NDVI at all sites in 2005 and 2006. It can be found that in 2005, UG79, UG99, and WG have minimum NDVI measurements at the beginning of the growing season and maximum measurements in August. However, the peak NDVI of site CG appeared in August, but appeared in July

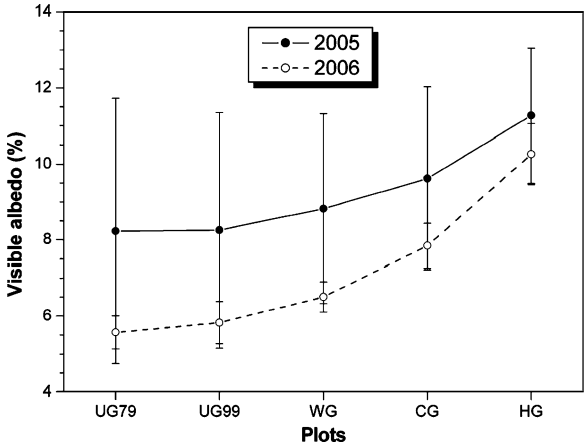

Fig. 6 Mean visible albedo (with standard deviation) in 2005 and 2006 at each site (UG79, UG99, WG, CG, and HG)

Table 2 Mean visible albedo and NDVI (with standard deviation) in 2005 and 2006 at five measurement sites

	Visible albedo		NDVI	
	2005	2006	2005	2006
UG79	0.082±0.035	0.056±0.0044	0.395±0.117	0.496±0.053
UG99	0.083±0.031	0.058±0.0055	0.323±0.124	0.445±0.060
WG	0.088±0.025	0.065±0.0040	0.332±0.075	0.416±0.049
CG	0.096±0.024	0.078±0.0059	0.311±0.072	0.316±0.055
HG	0.113±0.018	0.103±0.0080	0.293±0.050	0.332±0.047

for site HG; the lowest NDVI of these two sites were observed not at the beginning but at the end of the growing season, in contrast to that seen for the other sites. In addition, similar to the visible albedo, HG has the smallest NDVI variation among the five sites.

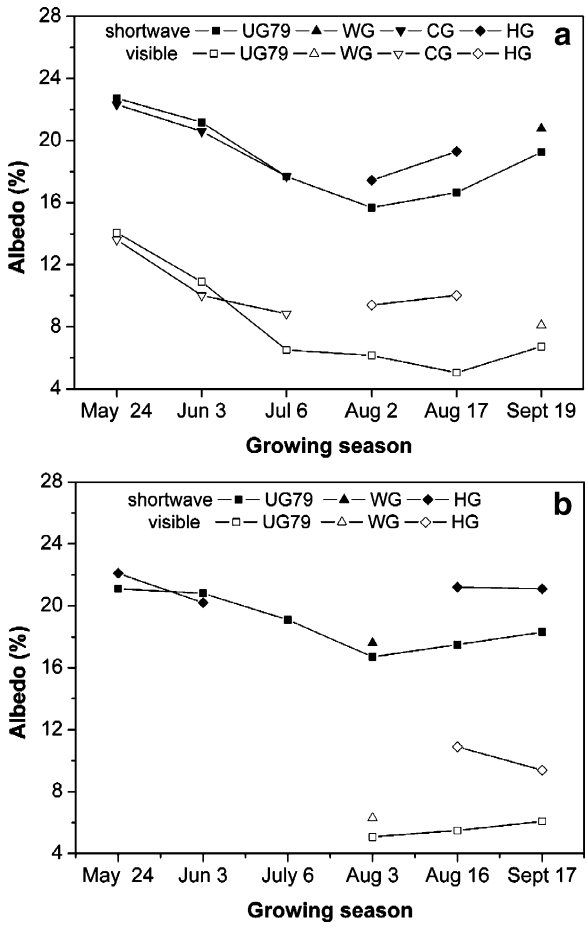

Fig. 7 Comparison of visible albedo measured by spectrometer and total shortwave albedo measured by pyranometer installed at EC tower in 2005 (**a**) and 2006 (**b**) (here visible albedo is only showing during the total shortwave albedo measurements)

Using the NDVI values on June 3, July 6, August 2, August 17, and September 19, the monthly growth situations are estimated.

From June to July, all sites except CG had good growth. NDVI increases 38.7%, 71.4%, 14.8% and 20% at sites UG79, UG99, WG and HG, respectively. From July to August, sites UG79, UG99, and WG

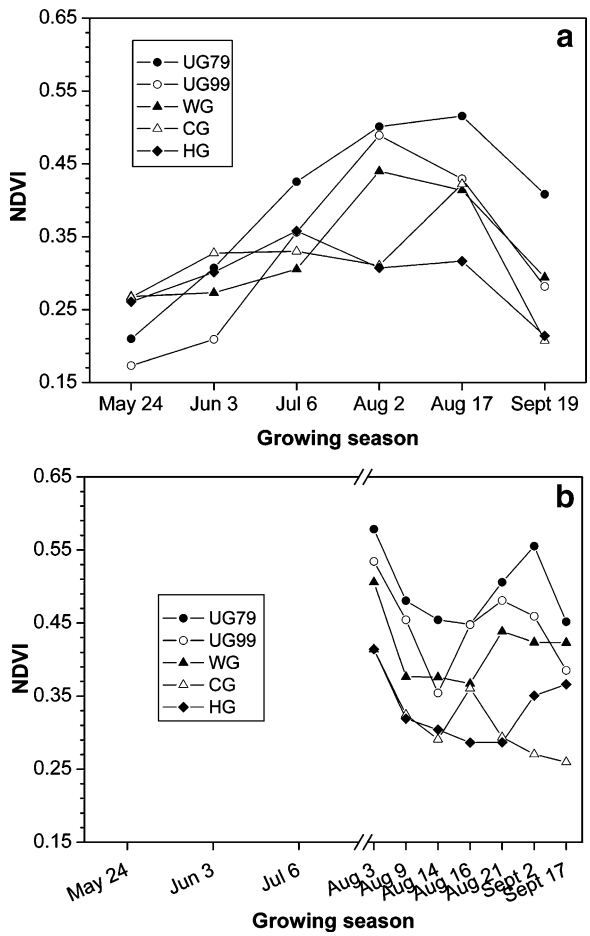

Fig. 8 Seasonal variation of NDVI in 2005 (**a**) and 2006 (**b**) at each site (UG79, UG99, WG, CG, and HG)

kept growing (16.3%, 36.1%, and 41.9%, respectively), but at sites CG and HG, NDVI decreased (−0.06% and −16.7%, respectively; as the grass growth from June to July was rather poor at CG site, the NDVI decrease from July to August was not large and hence the difference is very small). From late August on, NDVI decreased. The decrease of NDVI from August 17 to September 19 was above 20% at all five sites and even higher at sites CG and HG (21.2%, 34.8%, 34.1%, 50.0% and 37.5%, respectively).

In 2006, peak NDVI appeared at the beginning of August (August 3) at all sites and was higher than that for the corresponding time period in 2005 (August 2, differences are 0.08, 0.04, 0.07, 0.10, and 0.10, respectively). The reason could be due to the relatively high precipitation from May to July 2006 (136.2 mm, 50.9 mm higher than 2005). Based on the differences at each site, it can be seen that the NDVI at the grazed sites is more sensitive to precipitation than at the ungrazed sites.

In addition to the peak value, there was a secondary peak NDVI found at all sites. For sites UG79, UG99 and WG, this peak occurred around August 21 to September 2. The reason could be due to the rainfall from August 19 to 20 (9.8 mm) and August 30 to September 1 (10.9 mm). The secondary peak NDVI at site CG appeared on August 16, in contrast to the other sites, considering the rainfall influences. This difference might be caused by measurement errors, due to the site's heavily grazed status and heterogeneous characteristics in 2006. The NDVI at site HG did not increase on August 21 after the short period of rainfall, as seen at sites UG79, UG99, and WG, but after the rainfall around September 1, which is possibly due to the much lower rainfall, the dry soil and the poor status of the vegetation (low percent green cover) in August.

After the heavy snowfall around September 7, the NDVI at the five sites was higher than that for the corresponding time period in 2005 (September 19, difference is 0.04, 0.10, 0.13, 0.05, and 0.15, respectively). Site HG showed an increase in NDVI, even after the snowfall. Measurements showed that soil moisture at site HG after the snowfall was higher than at site UG79; this relationship being opposite during the entire growing season. The reason could be that the simple vegetation structure and the degradation at site HG aided in rapid snow melting and infiltration into the soil, rather than being trapped and sublimating (as interception loss), as was the case at site UG79.

Figure 9 and Table 2 show the average NDVI at the five sites in 2005 and 2006. The differences between the sites are distinct, and a trend is obvious: heavier grazing is associated with lower NDVI. Site UG79 had the highest mean NDVI among the five sites. The values at the other sites were 0.82, 0.84, 0.78, and 0.74 times the value of site UG79 in 2005, and 0.90, 0.84, 0.64, and 0.67 times the value of site UG79 in 2006. The slightly lower value at site UG99 in 2005 is due to the large percentage of standing dead vegetation, and the lower value at site CG in 2006 is due to heterogeneous characteristics. The mean NDVIs at the five sites were higher in 2006 than in 2005 and had smaller SD due to the short measurement period.

We used the derived NDVI in this study to investigate the NDVI and LAI relationship in the area (Fan et al 2009) and obtained sufficiently well-defined linear and exponential relationships, respectively. Here, we also analyse the relationship between NDVI and the total shortwave albedo measured by the pyranometer installed at EC tower (Fig. 7) and obtain a linear relationship between the two parameters:

$$Albedo = 0.252 - 0.158NDVI \quad (R = -0.82, \quad N = 24) \tag{3}$$

If two outliers are removed at sites CG and HG (caused by heterogeneity at the two grazed sites and

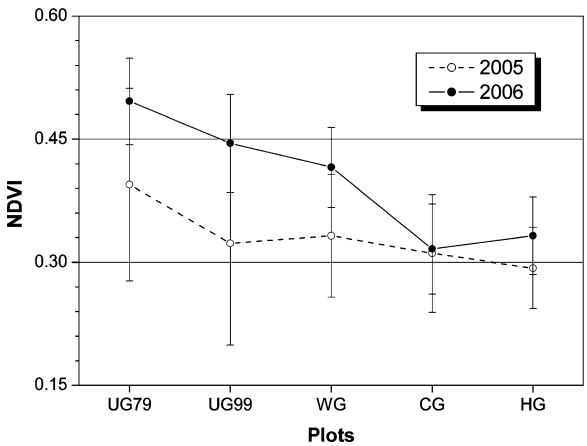

Fig. 9 Mean NDVI (with standard deviation) in 2005 and 2006 at each site (UG79, UG99, WG, CG, and HG)

poor weather conditions in 2005, respectively) the correlation changes to:

$$Albedo = 0.261 - 0.175NDVI \quad (R = -0.92, \quad N = 22) \tag{4}$$

Thus, approximately 85% (R^2=0.85) of the variability in total shortwave albedo is explained by NDVI and vice versa. Therefore, NDVI spectrometer measurements and total shortwave albedo pyranometer measurements are interchangeable when addressing different grazing intensities.

Discussion and conclusions

In this paper, we conducted spectral reflectance measurement campaigns at five different grazing intensity grasslands in Inner Mongolia, China, in 2005 and 2006 to study the grazing effects on spectral reflectance seasonal dynamics and interannual variations. The major findings are summarised below.

Grazing effects on seasonal dynamics of spectral reflectance

(1) Grazing effects influences the shape of the reflectance spectrum. With no grazing occurring for a long time, as occurred in sites UG79 and UG99, the chlorophyll red edge change and peak shoulder in the green band were pronounced during the mature period. However, when disturbed by grazing, as occurred in sites CG and HG, these spectrum phenomena were blurred and disappeared rapidly in September. As the chlorophyll red edge and peak shoulder in the green band are linked to chlorophyll content in the vegetation, grazing affects the vegetation and then influences the spectrum change.

(2) Site UG79 had the biggest visible albedo variation during the growing season; by contrast, HG had the smallest change but always had the highest value during the entire season. This indicates that disturbing a site with grazing, particularly heavy grazing, results in poor vegetation growth and a low percentage of green cover; as a result, the surface reflectance includes much more soil information. In addition, after long-term heavy grazing (30 years, Archer 2004b), the vegetation at site HG has degraded to a certain extent, the composition of vegetation types has changed, and soil contents and structure have also changed. These features may also lead to high visible albedo.

(3) The visible albedo of the five differently grazed sites showed small differences at the beginning of the growing period but presented large differences in late August. This result clearly shows the grazing effects on the seasonal dynamics of spectral reflectance.

(4) Grazing effects change the seasonal pattern of NDVI.

From July to August, the NDVI at the CG and HG sites decreased earlier than at the other ungrazed sites, and site HG even had the early NDVI peak in July rather than in August, in contrast to the other sites. From late August until late September, the decrease in NDVI at sites CG and HG was higher than at the other sites; therefore, these two sites had minimum NDVI values at the end of the season, but the other ungrazed sites had minimum values at the beginning of the growing season.

The reason for NDVI appearing earlier at site HG could be that overgrazing hinders vegetation growth over a threshold level. Additionally, as discussed above, the composition of vegetation types has changed. The growing pattern may also affect the peak time of biomass.

(5) By disturbing a site with heavy grazing, the NDVI at site HG also shows minor variations, such as the visible albedo during the entire growing period.

Grazing effects on interannual variation of spectral reflectance

We determined spectral reflectance in 2005 and 2006. From meteorological data, we know that these 2 years had minor differences in temperature but large differences in precipitation, especially in September. By comparing the corresponding time values in these two years, we identified some aspects of grazing effects on surface spectral reflectance interannual variations with regard to precipitation.

(1) Visible albedo and NDVI analyses both showed that grazed sites (CG and HC) are more sensitive

to precipitation. After the heavy snowfall in September 2006, the visible albedo at sites CG and HG were much lower than that for the corresponding time period in 2005, and their NDVI values were much higher than that for the corresponding time period in 2005.

(2) Site HG showed unique phenomena with regard to precipitation. First, this site did not show the secondary peak NDVI value like the other sites after a short period of rainfall in August 2006. Second, HG showed an increase in NDVI, even after the snowfall. These unique reactions to snowfall further suggest degradation at site HG by heavy grazing treatment.

From this study, we also know that visible albedo, measured by the spectrophotometer, and total shortwave albedo, measured by the pyranometer installed at EC tower, are well correlated (R^2 of 0.69 and 0.88 in 2005 and 2006, respectively). In addition, we obtained a well-defined linear relationship between NDVI and total shortwave albedo (Eq. 4). Therefore, NDVI spectrometer measurements and total shortwave albedo pyranometer measurements are interchangeable when addressing different grazing intensities.

Acknowledgements This research was supported by the German Research Foundation (Deutsche Forschungsgemeinschaft, DFG) within the Research Unit FOR 536 MAGIM ("Matter Fluxes in Grasslands of Inner Mongolia as influenced by Stocking Rate") by grant BE 1721/7. Part of the work was performed at Peking University under the supervision of Prof. Shuhua Liu. We thank PD Dr. Franz H. Berger for study support in the initial stage of this project. We are also grateful to IMGERS for providing precipitation data.

References

Archer N (2004a) Summary of geostatistical sites for the MAGIM project. www.magim.net/intranet

Archer N (2004b) General description and information about the experimental area. www.magim.net/intranet

Boegh E, Soegaard H, Broge N, Hasager CB, Jensen NO, Schelde K, Thomsen A (2002) Airborne multispectral data for quantifying leaf area index, nitrogen concentration, and photosynthetic efficiency in agriculture. Remote Sens Environ 81:179–193

Colombo R, Bellingeri D, Fasolini D, Marino CM (2003) Retrieval of leaf area index in different vegetation types using high resolution satellite data. Remote Sens Environ 86:120–131

Duchon CE, Hamm KG (2006) Broadband albedo observations in the southern Great Plains. J Appl Meteorol Climatol 45:210–235

Elvidge CD, Chen Zh (1995) Comparison of broad-band and narrow-band red and near-infrared vegetation indices. Remote Sens Environ 54:38–48

Fan L, Gao Y, Brück H, Bernhofer Ch (2009) Investigating the relationship between NDVI and LAI in semi-arid grassland in Inner Mongolia using in situ measurements. Theor Appl Climatol 95:151–156

Gates DM, Gates HJ, Gates JC, Gates VR (1965) Spectral properties of plants. Appl Opt 4(1):11–20

Guo XL, Price P, Stiles J (2003) Grasslands discriminant analysis using Landsat TM single and multitemporal data. Photogrammetric Eng Remote Sens 69(11):1255–1262

Higuchi A, Kondoh A, Kishi S (2000) Relationship among the surface albedo, spectral reflectance of canopy, and evaporative fraction at grassland and paddy field. Remote Sens Land Surf Characterisation 26(7):1043–1046

Houborg R, Boegh E (2008) Mapping leaf chlorophyll and leaf area index using inverse and forward canopy reflectance modeling and SPOT reflectance data. Remote Sens Environ 112:186–202

Huang Z, Turner BJ, Dury SJ, Wallis IR, Foley WJ (2004) Estimating foliage nitrogen concentration from HYMAP data using continuum removal analysis. Remote Sens Environ 93:18–29

Jackson RD, Slater PN, Pinter PJ (1983) Discrimination of growth and water stress in wheat by various vegetation indices through a clear and a turbid atmosphere. Remote Sens Environ 13:187–208

Jiang S (1985) An introduction on the Inner Mongolia grassland ecosystem research station. In: the Chinese Academy of Sciences (ed) Inner Mongolia grassland ecosystem research station. Research on Grassland Ecosystem (No.1). Science Press, Beijing, pp 1–11 [in Chinese]

Kawamura K, Akiyama T, Yokota H, Tsutsumi M, Yasuda T, Watanabe O, Wang SP (2005) Quantifying grazing intensities using geographic information systems and satellite remote sensing in the Xilingol steppe region, Inner Mongolia, China. Agric Ecosyst Environ 107(1):83–93

Knyazikhin Y, Martonchik JV, Diner DJ, Myneni RB, Verstraete M, Pinty B et al (1998) Estimation of vegetation canopy leaf area index and fraction of absorbed photosynthetically active radiation from atmosphere corrected MISR data. J Geophys Res 103(D24):32239–32256

Leblon B, Guerif M, Baret F (1991) The use of remotely sensed data in estimate of PAR use efficiency and biomass production of flooded rice. Remote Sens Environ 38:147–158

Li B, Yong Sh, Li Y, Liu Y (1990) Grassland in China, 1st edn. Science Press, Beijing, pp 87–168

Li SG, Harazono Y, Oikawa T, Zhao HL, He ZY, Chang XL (2000) Grassland desertification by grazing and the resulting micrometeorological changes in Inner Mongolia. Agric For Meteorol 102:125–137

Liang Sh (2000) Narrowband to broadband conversions of land surface albedo I Validation. Remote Sens Environ 76:213–238

Liang Sh, Fang H, Chen M, Shuey CJ, Walthall C, Daughtry C, Morisette J, Schaaf C, Strahler A (2002a) Validating MODIS land surface reflectance and albedo products: methods and preliminary results. Remote Sens Environ 83:149–162

Liang Sh, Shuey CJ, Russ AL, Fang H, Chen M, Walthall CL, Daughtry CST, JrR H (2002b) Narrowband to broadband

conversions of land surface albedo: II. Validation. Remote Sens Environ 84:25–41

Liu Y, Zha Y, Gao J, Ni S (2004) Assessment of grassland degradation near Lake Qinghai, West China, using Landsat TM and in situ reflectance spectra data. Int J Remote Sens 25(20):4177–4189

Pineiro G, Oesterheld M, Paruelo JM (2006) Seasonal variation in aboveground production and radiation-use efficiency of temperate rangelands estimated through remote sensing. Ecosystems 9(3):357–373

Price KP, Guo XL, Stiles JM (2002) Optimal Landsat TM band combinations and vegetation indices for discrimination of six grassland types in eastern Kansas. Int J Remote Sens 23(23):5031–5042

Tucker CJ (1979) Red and photographic infrared linear combinations for monitoring vegetation. Remote Sens Environ 8:127–150

Vaesen K, Gilliams S, Nackaerts K, Coppin P (2001) Ground-measured spectral signatures as indicators of ground cover and leaf area index: the case of paddy rice. Field Crops Res 69:13–25

Wang YR (1998) A comparative analysis between the seasonal multispectral reflectance and biomass of Leymus chinensis steppe in different grazing degradation intensity. Acta Scientiarum Naturalium Universitatis NeiMongol 29 (1):102–108 [in Chinese with English abstract]

Wang YR (2001) The influence of different grazing intensity on the near-ground spectral reflectance of Leymus chinensis steppe. Grassland of China 23(2):1–6 [in Chinese with English abstract]

Yoder BJ, Pettigrew-Crosby RE (1995) Predicting nitrogen and chlorophyll content and concentration from reflectance spectra (400–2500 nm) at leaf and canopy scales. Remote Sens Environ 53:199–211